Strain-modulated band structure and high harmonic generations in two-dimensional MoS_2

Yuchen Sun

University of Cambridge, The Old Schools, Trinity Lane, Cambridge, CB2 1TN, United Kingdom

ys580@cam.ac.uk

Abstract. Two-dimensional (2D) condensed matter is a material that is restricted in one direction while being periodic in the other. Since the restricted size of 2D materials is comparable to the wavelength of electrons, a quantum confinement effect may occur. Moreover, the absence of periodicity provides weak screening in 2D materials, which brings novel physical properties such as the quantum well, which is widely applied in quantum information, and the fine absorption structures in graphene. Among the 2D materials, the monolayer transition metal chalcogenides represented by MoS_2 have attracted wide attention due to the direct band gap in the visible light region (1.8 eV) and valley polarizations, which are prospective for solar cells as well as photoelectric devices. High-harmonic generation (HHG) is a strong non-linear process during which a high-energy laser impulse is applied to materials and high-harmonic radiations are yielded. As a typical ultrafast dynamic, HHG has important applications in laser generation, such as EUV lithographic metrology and high-resolution coherent imaging. According to the Bloch oscillation model, HHG is highly dependent on band structure. Here, we report the strain-dependent HHG dynamics in MoS_2. Further investigation reveals that the strain-dependence of HHG is caused by band modulation under different strains, which is dominant during HHG. Our research sheds light on ways to achieve effective modulations in ultrafast dynamics, implying an all-optical measurement band structure in strained materials.

Keywords: Molybdenum disulfide (MoS_2), High harmonic generation, Two-dimensional material, Bloch model, Strain.

1. Introduction

Since the discovery of Nobel prize material graphene in 2004 [1], two-dimensional (2D) materials have piqued the interest of both fundamental physicists and material scientists [2]. Because of their monoatomic thickness in one direction, 2D materials exhibit inefficient screening and quantum confinement effects, resulting in enhanced interactions between particles at the quasiparticle level. The effective interactions bring 2D materials a lot of extraordinary properties, including high thermal/electrical conductivity, novel optical response and improved electron-phonon couplings [3-6], which show wide perspectives on the applications of photoelectric devices and solar cells [7-10]. In the huge 2D material family, the monolayer MoS_2 magnifies itself owing to the visible band gap (~1.8 eV) and valley selectivity, whose band structures are wildly explored and modulated for carrier dynamic engineering [11-16].

High-harmonic generation (HHG), a nonlinear process that generates high energy and ultrafast coherent radiations under strong laser illumination, has been shown to be effective in MoS_2 and sensitive to band curvatures [17-19]. Considering the great importance of HHG in probing solid properties and attosecond pulse generation [20-26], it is necessary to find out the electric mechanism of HHG. Unfortunately, the relationship between the band and HHG is still unclear. In this letter, based on the Bloch oscillation model, we investigate the field dependence of HHG in MoS_2 with different band structures driven by strains. A sensitive, strain-dependent HHG is revealed, which comes from the modulated band structure as well as the electron scatting dynamics on it. Our results will benefit further understanding and application of HHG in condensed phases and quantum materials.

Due to their fancy properties, which are different from bulk materials, 2D materials are restricted in one direction, and a quantum tunneling effect may occur in the materials. It has a lot of extraordinary properties, such as high thermal conductivity and high electrical conductivity. These properties give it wide applications in transistors and solar cells. MoS_2 is also a typical 2D material. The S-Mo-S sandwiches are bonded by van der Waals forces. This weak interaction gives us a better opportunity to modify its structure. It also has a direct band gap of 1.8 eV when the layer number decreases, which solves the gapless problem of graphene.

High-harmonic generation (HHG) is a strong non-linear process during which a high-energy laser impulse is applied to materials and high-harmonic radiations are yielded. It can be understood through the three-step model, which includes tunnel ionization, free acceleration, and recombination. As a typically ultrafast dynamic, high-harmonic generation has important applications in laser generation, such as According to the Bloch oscillation model, HHG is highly dependent on band structures. Former researchers investigated the relationship between the intensity of the laser impulse and the intensity of HHG in SiO2 films [21]. However, the relationship between the energy band and HHG is not clear, and the change in HHG under different strains has not been researched either. Here, we investigate the relationship between HHG and the energy band and strain-dependent HHG dynamics in MoS_2.

2. Methods

In this paper, the dispersion of valence and conduction bands in MoS_2 along Γ-K and Γ-M direction is investigated under the isotopic strains e=-2%, 0%, 2%, and 8% [27]. The following formula represents the relationship between energy E(k) and crystal momentum k [21]:

$$E(k) = \sum_{n=1}^{n_{max}} \varepsilon_n \cos(nka) \tag{1}$$

which is essentially a Fourier series of the energy band E(k), with only cos terms remaining because the band is symmetric by Γ. ε_n is the Fourier coefficient and a is the lattice constant. The group velocity of electrons can be written as $v_g = \frac{dE(k)}{dk}$ and the pulse for an electric field at frequency ω_L is $E(t) = E_0 sin(\omega_L t + \varphi)$. Then the Bloch model is used to derive the relationship between the intensity of high-harmonic generation and the electric field. The Bloch oscillation is $k(t) = \frac{E_0}{\omega_L} cos(\omega_L t + \varphi)$. So the current is

$$j \sim v_g = \sum_{n=1}^{n_{max}} n\varepsilon_n \text{asin}\,(n\frac{E_0}{\omega_L}\cos(\omega_L t + \beta)\,\alpha \tag{2}$$

The source of HHG radiation is given by time derivative of the current and thus the intensity of HHG is $I(\omega) \propto |\frac{\partial j}{\partial t}|^2$ and in the frequency domain it is $I(\omega) \propto |\omega j(\omega)|^2$. Using Jacobi-Anger expansion, the intensity dependence of the Nth order harmonic is proportional to [21,28]:

$$I_N \propto (N\omega_L)^2 \left| \sum_{n=1}^{n_{max}} n\varepsilon_n J_N \left[\frac{eF_0 a}{\hbar\omega_L} \right] \right|^2 \quad (3)$$

where $J_N[z]$ is the Bessel function of the first kind of order N.

3. Results and discussions

Given the mirror symmetry of MoS_2, both the conduction and valence bands in pristine MoS_2 exhibit obvious symmetry along the K-Γ-K direction, as shown in Fig. 1 (a). The valence band (VB) shows a typical parabolic dispersion with a global minimum at Γ point, while the conduction band (CB) has a more complex dispersion where two local maximums appear near the midpoints of Γ and K. The band structures of VB and CB yield a band gap of around 1.8 eV at the Γ point.

Under weak strain (E = 2%), the band width of CB is enhanced, and the band modulation on VB is moderate. This trend becomes more obvious with the uniaxial strain (Fig. 4): the band widths of both VB and CB are increased, and the effective mass is modulated. As the strain increases (E = 8%), the bands show significant changes where two local minimums emerge near the midpoints of Γ and K while CB degenerates into a parabola-like dispersion. However, the situation becomes different when the strain direction reverses (E = -2%), both the VB and CB show simple parabolic dispersion.

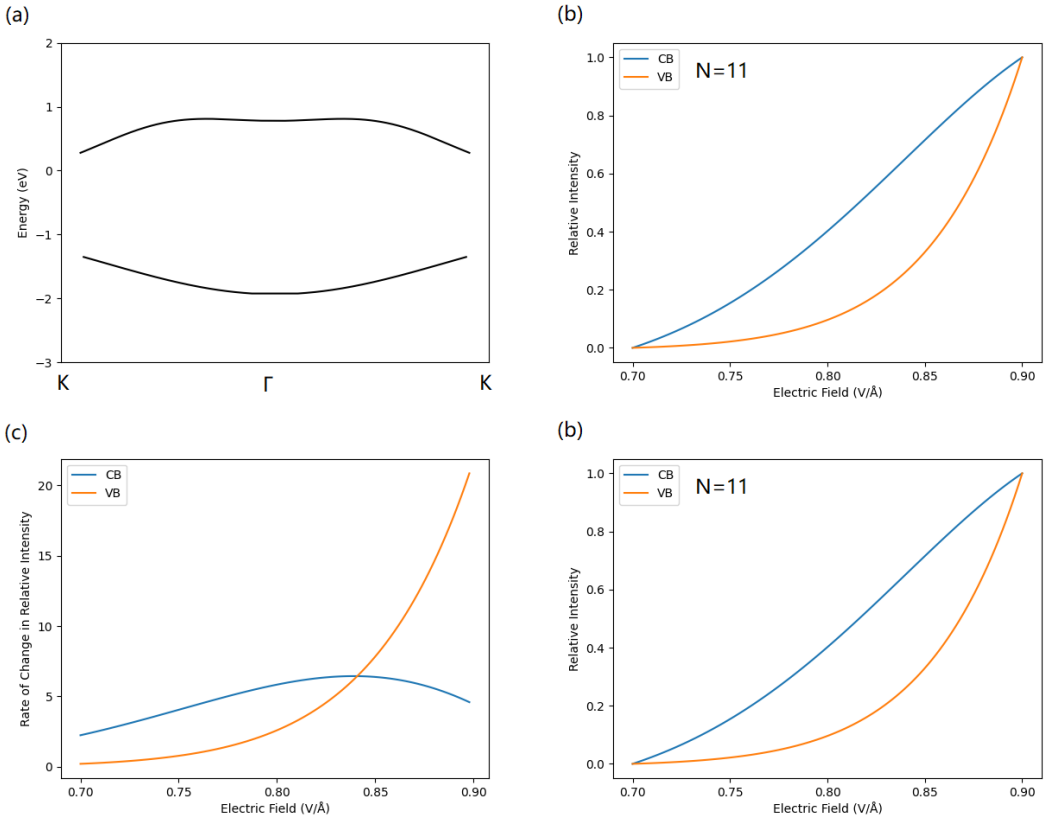

Figure 1. (a) The band structure of pristine MoS_2 along K-Γ-K direction. (b) The harmonic intensity at the 11th order as a function of electric field strength driven from the band structure in (a). (c) The rate of change of harmonic intensity at the 11th order as a function of electric field strength. (d) The harmonic intensity at the 15th order as a function of electric field strength.

Along with the band curvature change is the band gap, whose evolution is shown in Fig. 5. The band gap is proportional to the strain intensity, showing monotonic linear behavior. The results indicate the sensitive strain-dependence of the band in MoS_2, due to the change in lattice structure and charge

distribution induced by strains. The strain modulation further affects the nonlinear electronic dynamics, i.e., the HHG process, according to the Bloch model, which connects the HHG intensity with the band curvatures.

As shown in Figs. 1-4, within a certain range of field strength (0.5-1.0 V/A), both the HHG intensity and its gradient show a proportional relationship with the strength of the laser electric field for almost all the strain cases (the anomalous decrease for E > 0.65 V/A under E = -2% strain is due to the oscillation behavior of the Bessel function, which implies an intensity competition caused by different harmonic interference), indicating the nonlinear dynamics of electrons beyond perturbation. It is interesting and constructive to note that the shape of band dispersion has an effect on HHG behaviors: the HHG produced by parabola-like bands tends to increase slowly at low field intensity while growing faster at high field intensity (e.g., the HHG of VB under E = 0%, 2%, and CB under E = 8%). By contrast, the bands with more complex curvatures prefer to yield HHG with a uniform change rate at different field strengths. Furthermore, the band width also shows influences on the HHG process, where wider bands would induce uneven growth harmonics. This band-dispersion dependence of HHG reveals the sensitive relationship between nonlinear dynamics and electronic structure in strong field, which can be used in turn to determine the solid band structure under different external modulations by an all-optical measurement technology.

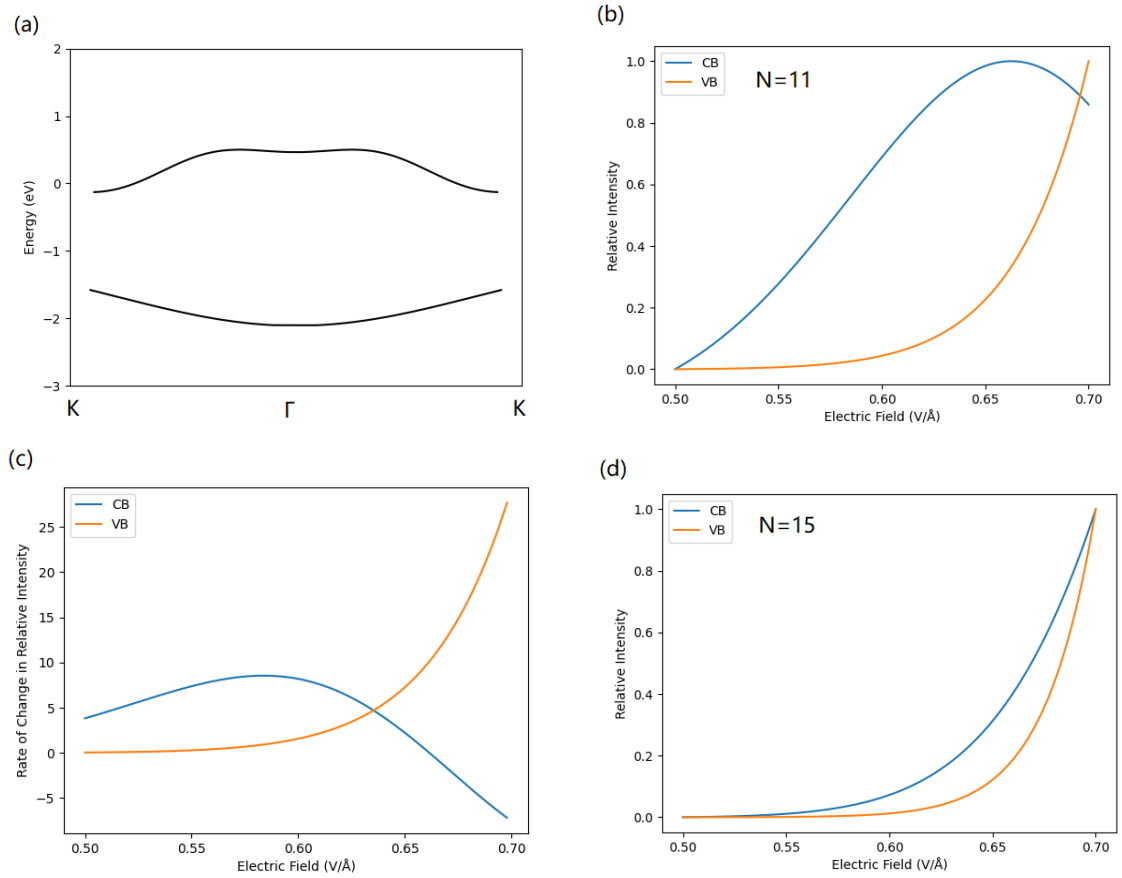

Figure 2. (a) The band structure of under a E=2% isotropic strain along K-Γ-K direction. (b) The harmonic intensity at the 11th order as a function of electric field strength driven from the band structure in (a). (c) The rate of change of harmonic intensity at the 11th order as a function of electric field strength. (d) The harmonic intensity at the 15th order as a function of electric field strength.

As shown in Figs. 1-4 and 6-7, the relationship between the intensity of HHG and the order is also investigated. For HHG of low order (N = 11), the intensity increases at a relatively uniform rate. For

HHG of higher order (N = 15), the intensity increases slowly for a small electric field and grows fast for a strong electric field. This may come from the proportional relationship between the harmonic intensity and the corresponding order, i.e., I∝N2. The nonmonotonic field dependence of the Bessel function may also come into play. This property also implies that the high-order harmonics would be more remarkable to be detected, while the low-order harmonics may strongly signal themselves with weak field strength.

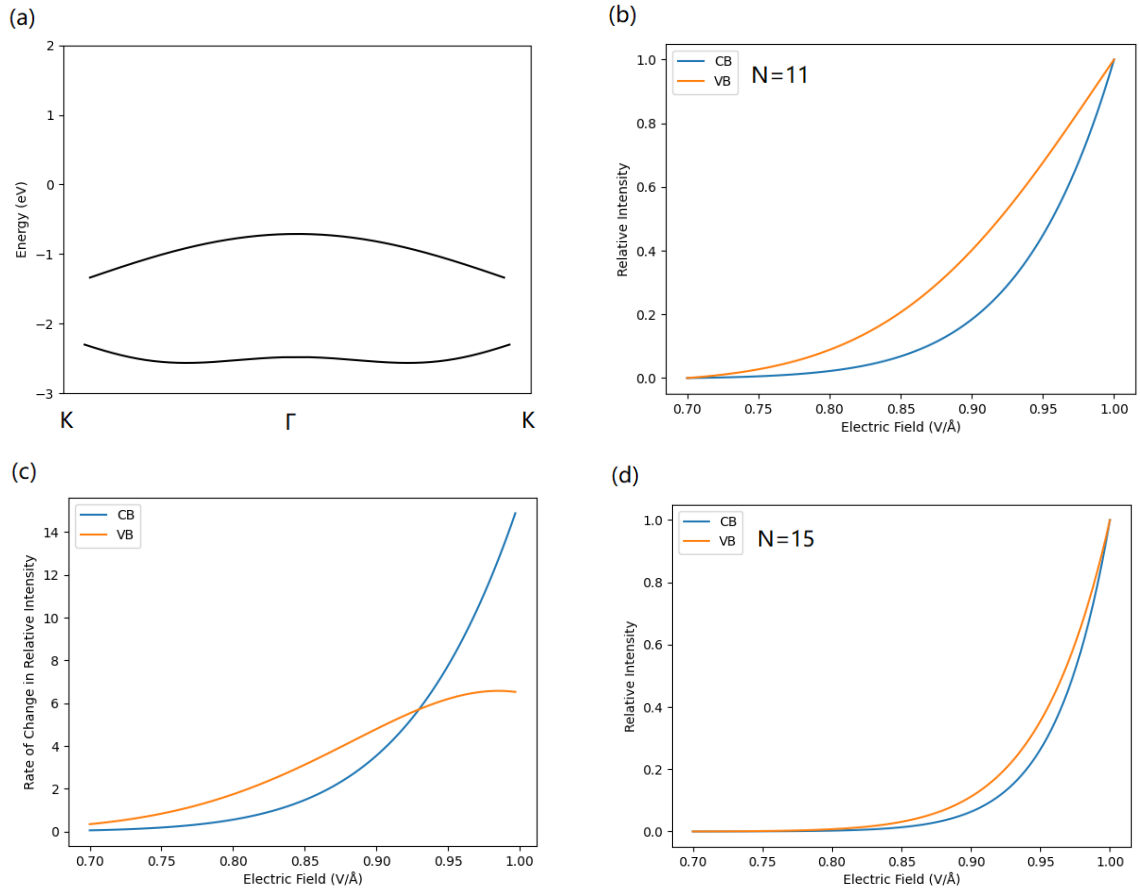

Figure 3. (a) The band structure of under a E=8% isotropic strain along K-Γ-K direction. (b) The harmonic intensity at the 11th order as a function of electric field strength driven from the band structure in (a). (c) The rate of change of harmonic intensity at the 11th order as a function of electric field strength. (d) The harmonic intensity at the 15th order as a function of electric field strength.

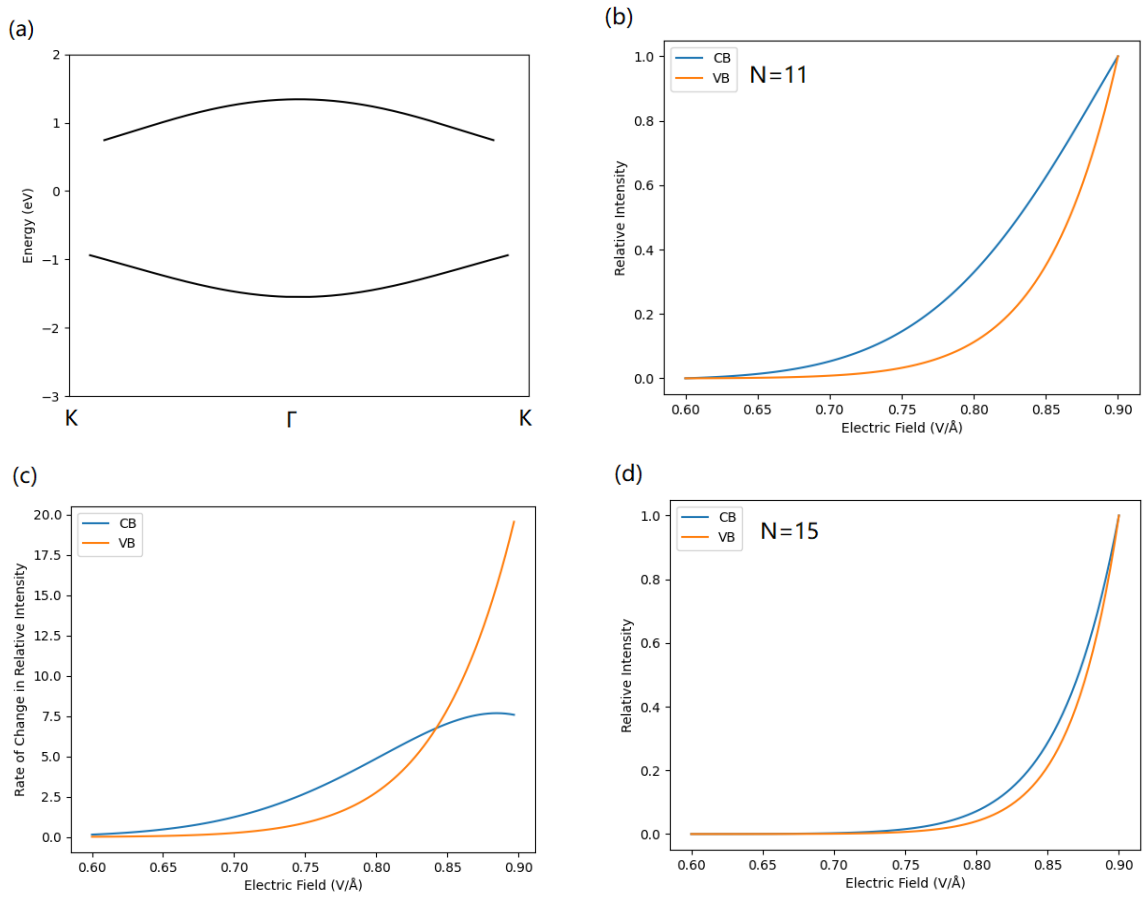

Figure 4. (a) The band structure of under a E=-2% isotropic strain along K-Γ-K direction. (b) The harmonic intensity at the 11th order as a function of electric field strength driven from the band structure in (a). (c) The rate of change of harmonic intensity at the 11th order as a function of electric field strength. (d) The harmonic intensity at the 15th order as a function of electric field strength.

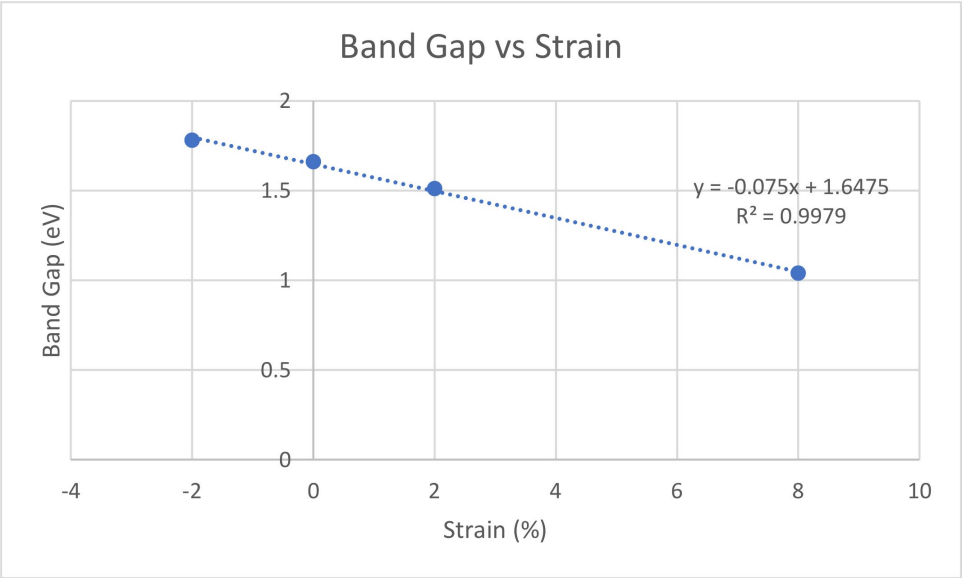

Figure 5. Relationship between band gap of monolayer MoS_2 and strain.

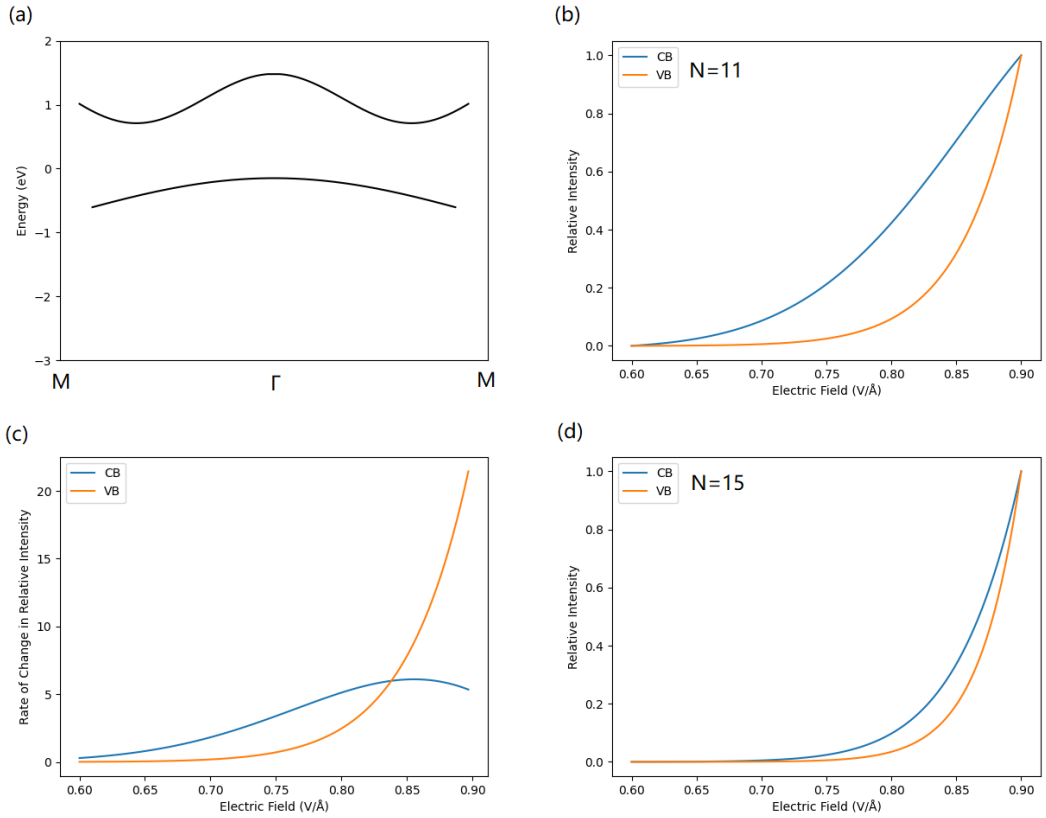

Figure 6. The band structure along K-Γ-K direction of MoS_2 under a E=8% x-axis strain. (b) The harmonic intensity at the 11th order as a function of electric field strength driven from the band structure in (a). (c) The rate of change of harmonic intensity at the 11th order as a function of electric field strength. (d) The harmonic intensity at the 15th order as a function of electric field strength.

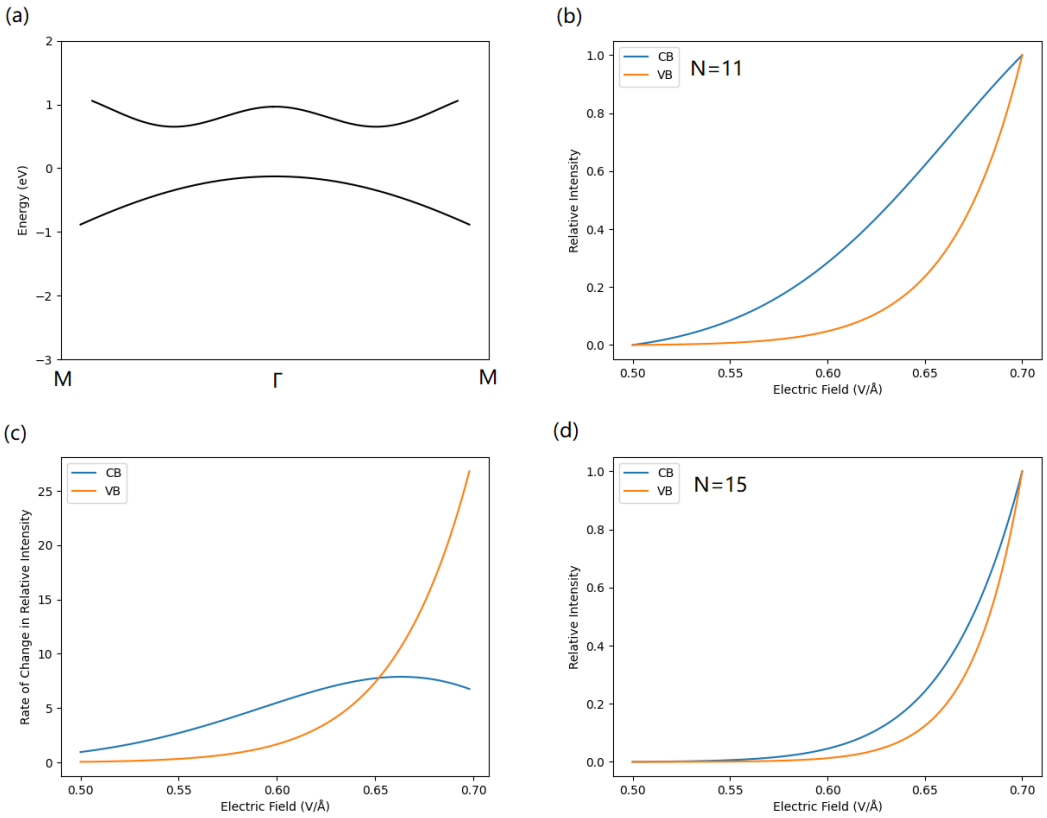

Figure 7. (a) The band structure along K-Γ-K direction of MoS_2 under a E=8% y-axis strain. (b) The harmonic intensity at the 11th order as a function of electric field strength driven from the band structure in (a). (c) The rate of change of harmonic intensity at the 11th order as a function of electric field strength. (d) The harmonic intensity at the 15th order as a function of electric field strength.

4. Conclusions

In this paper, we investigate the band curvature and resultant HHG of MoS_2 under different strains. We discover that the HHG produced by parabola-like bands increases slowly at low field intensity and rapidly at high field intensity. By contrast, the bands with more complex curvatures prefer to yield HHG with a uniform rate of change at different field strengths. Furthermore, we investigate the intensity of HHG in different orders. For HHGs of low order, the intensity increases at a relatively uniform rate. In the case of higher order HHG, the intensity increases slowly in a small electric field and rapidly in a strong electric field. Considering the strains provide good ways for band modulation, our results can be helpful in optical engineering since the nonlinear optical response is sensitive to the band curvature. On the other hand, our study also offers a good way to detect the tiny change in band curvature caused by HHG in the material.

References

[1] A. H. Castro Neto, F. Guinea, N. M. R. Peres, K. S. Novoselov, and A. K. Geim, The electronic properties of graphene, Rev. Mod. Phys. 81, 109 (2009).
[2] Geim, A., Grigorieva, I. Van der Waals heterostructures. Nature 499, 419–425 (2013).
[3] Jin, Z., Liao, Q., Fang, H. et al. A Revisit to High Thermoelectric Performance of Single-layer MoS_2. Sci Rep 5, 18342 (2015).
[4] Ermolaev, G.A., Stebunov, Y.V., Vyshnevyy, A.A. et al. Broadband optical properties of monolayer and bulk MoS_2. npj 2D Mater Appl 4, 21 (2020).

[5] Tan, Y., He, R., Cheng, C. et al. Polarization-dependent optical absorption of MoS_2 for refractive index sensing. Sci Rep 4, 7523 (2014).
[6] T. Sohier, E. Ponomarev, M. Gibertini, H. Berger, N. Marzari, N. Ubrig, and A. F. Morpurgo, Enhanced electron-phonon interaction in multivalley materials, Phys. Rev. X 9, 031019 (2019).
[7] A. Taffelli. Et al. MoS_2 Based Photodetectors: A Review 2021, 21(8), 2758.
[8] Zhao, Y., Ouyang, G. Thickness-dependent photoelectric properties of MoS_2/Si heterostructure solar cells. Sci Rep 9, 17381 (2019).
[9] Tsai, M. L., Su S. H., et al. Monolayer MoS_2 Heterojunction Solar Cells, ACS Nano 2014, 8, 8, 8317–8322.
[10] E.Fortin, W.M.Sears, Photovoltaic effect and optical absorption in MoS_2, Journal of Physics and Chemistry of Solids Volume 43, Issue 9, 1982, Pages 881-884
[11] Ryou, J., Kim, YS., KC, S. et al. Monolayer MoS_2 Bandgap Modulation by Dielectric Environments and Tunable Bandgap Transistors. Sci Rep 6, 29184 (2016).
[12] Tang, H., Neupane, B., Neupane, S. et al. Tunable band gaps and optical absorption properties of bent MoS_2 nanoribbons. Sci Rep 12, 3008 (2022).
[13] Mak, K., He, K., Shan, J. et al. Control of valley polarization in monolayer MoS_2 by optical helicity. Nature Nanotech 7, 494–498 (2012).
[14] Sie, E., McIver, J., Lee, YH. et al. Valley-selective optical Stark effect in monolayer WS2. Nature Mater 14, 290–294 (2015).
[15] Carrier and Polarization Dynamics in Monolayer MoS_2, Phys. Rev. Lett. 112, 047401 (2014).
[16] Ultrafast Carrier Thermalization and Cooling Dynamics in Few-Layer MoS_2, ACS Nano 2014, 8, 10, 10931–10940.
[17] Goulielmakis, E., Brabec, T. High harmonic generation in condensed matter. Nat. Photon. 16, 411–421 (2022).
[18] Ghimire, S., Reis, D.A. High-harmonic generation from solids. Nature Phys 15, 10–16 (2019).
[19] Liu, H., Li, Y., You, Y. et al. High-harmonic generation from an atomically thin semiconductor. Nature Phys 13, 262–265 (2017).
[20] von Hoegen, A., Mankowsky, R., Fechner, M., Först, M. & Cavalleri, A. Probing the interatomic potential of solids with strong-field nonlinear phononics. Nature 555, 79–82 (2018).
[21] Luu, T., Garg, M., Kruchinin, S. et al. Extreme ultraviolet high-harmonic spectroscopy of solids. Nature 521, 498–502 (2015).
[22] Probing ultrafast electron correlations in high harmonic generation, Phys. Rev. Research 2, 033037 (2020).
[23] Tran Trung Luu, H. J. Woerner, Measurement of the Berry curvature of solids using high-harmonic spectroscopy, Nature Communications, vol. 9 (1), 916, (2018).
[24] Ndabashimiye, G., Ghimire, S., Wu, M. et al. Solid-state harmonics beyond the atomic limit. Nature 534, 520–523 (2016).
[25] Li, J., Lu, J., Chew, A. et al. Attosecond science based on high harmonic generation from gases and solids. Nat Commun 11, 2748 (2020).
[26] Observation of a train of attosecond pulses from high harmonic generation. Science. 2001 Jun 1;292(5522):1689-92.
[27] Peng L., Wu X., et al. Strain-dependent electronic and magnetic properties of MoS_2 monolayer, bilayer, nanoribbons and nanotubes Phys. Chem. Chem. Phys., 2012, 14, 13035–13040.
[28] A. A. Lanin, E. A. Stepanov, A. B. Fedotov, and A. M. Zheltikov, Mapping the electron band structure by intraband high-harmonic generation in solids, Optica 4, 516 (2017).